European Conference on Optical Communication (ECOC) 2022 © Optica Publishing Group 2022

216 GBd Plasmonic Ferroelectric Modulator Monolithically Integrated on Silicon Nitride

Manuel Kohli(1), Daniel Chelladurai(1), Andreas Messner(1), Yannik Horst(1), David Moor(1), Joel Winiger(1), Tobias Blatter(1), Tatiana Buriakova(2), Clarissa Convertino(3), Felix Eltes(3), Michael Zervas(2), Yuriy Fedoryshyn(1), Ueli Koch(1), and Juerg Leuthold(1)

(1) ETH Zurich, Institute of Electromagnetic Fields (IEF), 8092 Zurich, Switzerland, manuel.kohli@ief.ee.ethz.ch, JuergLeuthold@ethz.ch

(2) Ligentec SA, 1024 Ecublens, Switzerland

(3) Lumiphase AG, 8802 Kilchberg, Switzerland

Abstract *We demonstrate a 216 GBd plasmonic ferroelectric modulator monolithically integrated with a foundry-produced silicon nitride platform. The combination of low-loss waveguiding, nanoscale plasmonics, and strong Pockels coefficients in barium titanate offers a platform for next-generation optical interconnect systems. ©2022 The Author(s)*

Introduction

Electro-optical modulators are essential building blocks in integrated optics to encode electrical data onto an optical carrier. These days, they should be able to encode 100 GBd and higher for next generation Tb/s links [1, 2]. They should feature lowest power consumption, a compact footprint [3], and ideally be compatible with the latest silicon nitride (SiN) platform.

Photonic modulators based on thin-film lithium niobate (LN) are among the best performing devices reported to date with up to 100 GBd in 2PAM [4], and 130 GBd at PS-400QAM [5], but have large footprints. The electro-optic (EO) interaction can be enhanced for smaller footprint by creating a slot filled with an organic EO material such as in silicon-organic-hybrid [6] and plasmonic-organic-hybrid (POH) devices [7, 8], where the metals simultaneously serve as electrodes and optical waveguides. POH modulators on the silicon-on-insulator platform offer micrometer-scale footprint [7], low energy consumption [8], high EO bandwidth beyond 500 GHz [9], and a symbol rate of 222 GBd on-off-keying [10]. An alternative to organics is offered by barium titanate (BTO) with a large r_{42} Pockels coefficient in thin film of > 900 pm/V [11] and its demonstrated functionality to elevated temperatures of 130° C in a compact, energy-efficient plasmonic BTO modulator on silicon [12]. In contrast, nitride based photonic platforms, such as silicon-oxynitride and SiN, are gaining interest in numerous applications [13, 14]. SiN is particularly attractive compared to silicon, as it offers lower propagation losses, a larger transparency window, lower thermal sensitivity, and the ability to handle higher optical input power [15-18]. In hybrid SiN approaches, SiN is deposited on another material such as LN. For instance, SiN on LN has already shown low voltage modulation [19] and data experiments up to 80 Gbit/s with a 30 GHz EO modulator [20]. Other examples of modulators on the SiN platform include graphene modulators showing 22 Gbit/s and 30 GHz 3dB bandwidth [21], or lead zirconium titanate with 40 Gbit/s and 30 GHz bandwidth [22]. Despite all advances, higher speeds on SiN have not yet been demonstrated.

In this work, the advantages offered by plasmonics, BTO as EO material, and low-loss SiN are combined to create a high-speed modulator that is monolithically integrated on a foundry-produced SiN platform. The plasmonic Mach-Zehnder modulator (MZM) operates at 216 GBd and features a flat frequency response beyond 70 GHz. For operation, it requires an offset bias of 3 V_{DC} and a drive voltage of 1.8 V_p. We demonstrate data modulation of 216 Gbit/s 2PAM and 256 Gbit/s 4PAM in an intensity-modulation/direct-detection (IM/DD) scheme with bit-error-ratios (BER) below the soft-decision forward error correction (SD-FEC) limit, and 160 Gbit/s 2PAM below the hard-decision FEC limit (HD-FEC).

Design and Fabrication

The plasmonic ferroelectric modulator on SiN consists of a Mach-Zehnder interferometer configuration with two phase modulators in push-pull mode. A schematic of a ferroelectric phase modulator is shown in Fig. 1(a).

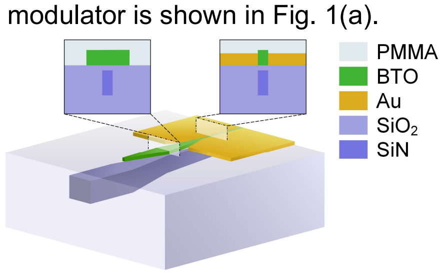

Fig. 1: Schematic and cross sections of a plasmonic ferroelectric phase modulator on SiN.

The MZM can be divided into three sections: the SiN waveguide, the BTO waveguide, and the active plasmonic section. Low-loss SiN is utilized as the main waveguiding layer for routing and splitting/combining of the optical signal. Efficient a-Si overlay gratings [23] couple light from a standard single-mode fiber to the SiN waveguide. The light is split on chip into the two arms of the MZM via a multi-mode interference coupler. Two steps are employed to couple light from the SiN waveguide to the active plasmonic section: first, an 80-µm-long tapered vertical directional coupler converts from the 800 nm × 800 nm SiN waveguide to the 1200 nm × 200 nm BTO waveguide. Second, a photonic-to-plasmonic converter couples the light from the BTO waveguide into the plasmonic slot by tapering the width of the metal slot. Each phase modulator has a slot width of 150 nm and a length of 15 µm. The simulated optical and electrical modes in the plasmonic slot are shown in Fig. 3(a). A field interaction factor [12, 24] of 0.96 was calculated, enabling a small footprint of the active section. The waveguide is oriented with a 45° angle relative to the crystal orientation of the BTO to maximize the in-device Pockels coefficient [12].

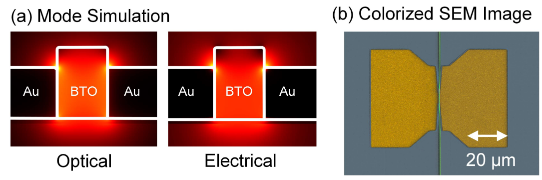

Fig. 3: (a) Simulated electric field profiles of the optical and electrical mode. (b) Colorized SEM image of a phase shifter

The modulator was fabricated on a combined SiN-BTO platform by backend-of-the-line (BEOL) processing. Definition of the SiN waveguides, followed by deposition of the oxide cladding, and surface planarization was done by Ligentec using its proprietary process. Next, the BTO was integrated on the wafer with patterned SiN with Lumiphase's proprietary process. Then, the BEOL fabrication processes include the BTO etching, and the a-Si deposition and etching for the overlay gratings. Electron-beam lithography was used to pattern the aforementioned structures. Subsequently, gold was deposited with electron-beam evaporation to form the plasmonic modulators. Finally, the chip was spin-coated with polymethylmethacrylate (PMMA) as cladding. Fig. 3(b) shows a colorized SEM image of a fabricated phase modulator in one MZM arm.

Results

The device was characterized optically and electro-optically, and tested in data modulation experiments.

The DC half-wave voltage ($V_{\pi,\mathrm{DC}}$= 3.2 V) of the MZM was determined by applying a DC bias. Fig. 2(c) shows the normalized and calibrated frequency response indicating a flat response up to 70 GHz. The high-frequency characterization of the modulator follows the method in [25]. The MZM has a V_π = 9.6 V at 40 GHz, showing a drop-off in comparison to DC. This arises from a lower electro-optical coefficient of BTO in plasmonic devices at higher frequencies [12, 26].

Fiber-to-fiber insertion loss (IL) below 10 dB is predicted by our simulations for ferroelectric plasmonic modulator. It comprises SiN to BTO coupling with losses < 0.1 dB, photonic-to-plasmonic conversion losses < 1 dB, and propagation losses of 0.3 dB/µm in the plasmonic section. However, we measure 29 dB fiber-to-fiber IL in this proof-of-principle device. These losses are attributed to approximately 3.5 dB per grating coupler and 0.75 dB per directional coupler between SiN and BTO waveguides (determined with reference devices). The propagation losses in the SiN and BTO are negligible due to the short propagation distance. Plasmonic propagation losses were measured with the cut-back method, yielding 0.5 dB/µm. Thus, the propagation loss of the 15 µm long device amounts to 7.5 dB. This leaves 6.5 dB loss per photonic-to-plasmonic converter. The IL exceeding the simulation is attributed to fabrication defects in this first fabrication run. For instance, improved metallization can decrease the IL by > 10 dB and potentially increase modulation efficiency for even smaller footprint.

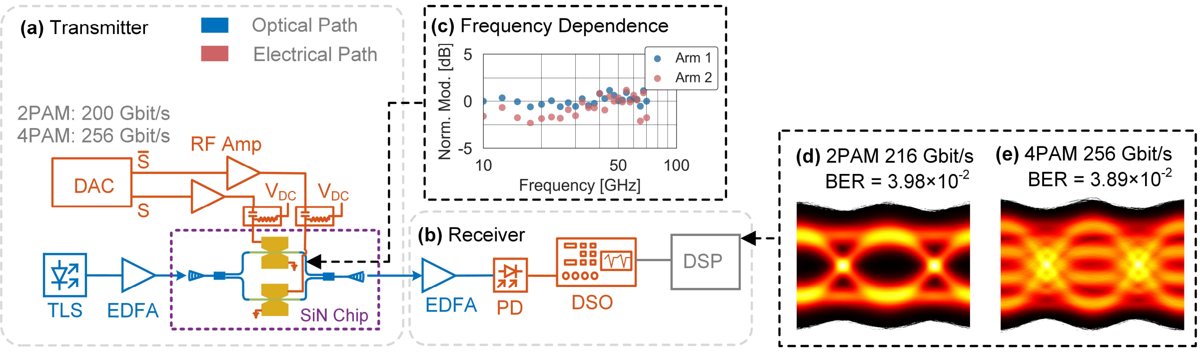

Fig. 2: Schematic of (a) the transmitter and (b) the receiver used for the data modulation experiment. (c) The MZM frequency response. (d) Eye diagram of 2PAM 216 Gbit/s and (d) of 4PAM 256 Gbit/s data modulation.

The data modulation experiment is illustrated in Fig. 2(a,b). At the transmitter, see Fig. 2(a), a 1557 nm optical carrier (18 dBm) from a tunable laser source (TLS) was coupled into the SiN chip. Electrical NRZ data signals were generated by a digital-to-analog converter (DAC) with symbol rates of up to 216 GBd and periodically repeated sequences of length $5 \cdot 10^5$. In the next step, the data signals were amplified to drive the MZM with voltage amplitudes of up to 1.8 V_p (at 128 GBd). A low DC bias of 3 V was applied to align the domains of BTO in the optimal direction enabled by the large poling fields induced in the nanoscale plasmonic slot. In the receiver, see Fig. 2(b), the optical data signal was amplified in an erbium-doped fiber amplifier (EDFA), filtered and fed to a photodetector (PD) for direct detection. The resulting baseband signal was captured by a real-time digital sampling oscilloscope (DSO) for offline digital signal processing (DSP). The full DSP consists of a timing recovery, a T/2-spaced linear equalization (LMS) with 151 taps, nonlinear equalization based on a 7-symbol pattern mapping and a 2nd order Volterra filter, and finally a T-spaced linear equalization with 151 taps. For the 216 GBd 2PAM signal, the filter taps of the linear equalizer and the pattern length of the nonlinear mapping were increased to 251 and 11, respectively. In Fig. 2(d), the received eye diagram of the 216 GBd 2PAM signal is depicted with a BER of $3.98 \cdot 10^{-2}$ and a signal-to-noise ratio (SNR) of 6.2 dB. The eye diagram of the 128 GBd 4PAM signal is shown in Fig. 2(e) with a BER of $3.89 \cdot 10^{-2}$ and SNR of 11.43 dB. The BER of both signals is below the SD-FEC limit. In Fig. 4, one can see the dependence of the measured BER on the transmitted symbol rate. For symbol rates < 128 GBd, the DSP can be simplified to a single linear equalization stage with 151 taps to achieve a comparable BER.

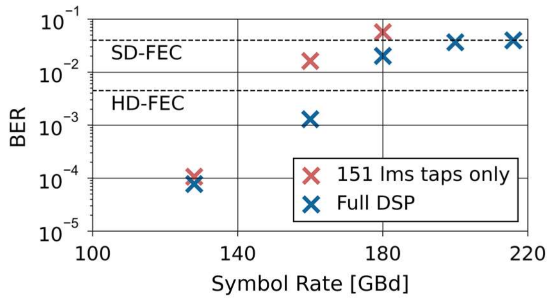

Fig. 4: The dependence of BER on the transmitted symbol rate for 2PAM modulation format.

Conclusions

A high-speed plasmonic ferroelectric modulator has been introduced, that is integrated on a low-loss SiN platform. The monolithic integration combines the advantages of highly nonlinear thin-film BTO with ultra-fast plasmonics, enabling a flat frequency response beyond 70 GHz. The modulator shows a DC voltage-length product of 45 Vµm and is suitable for high-speed data transmission. 2PAM has been demonstrated at 216 Gbit/s and 4PAM at 256 Gbit/s with BERs below the SD-FEC limit. 2PAM 160 Gbit/s operation with BER below the HD-FEC limit has been shown. The combination of inorganic electro-optic material with SiN paves the way for a next-generation energy-efficient active SiN platform.

Acknowledgements

This work was funded by the EC H2020 projects NEBULA (871658), PlasmoniAC (871391), and NEoteRIC (871330). We thank the cleanroom operations team of the Binnig and Rohrer Nanotechnology Center (BRNC) for their help and support. Measurements in this study have been recorded with the free and open-source laboratory automation software LabExT, available at https://github.com/labext/labext.

References

[1] A. Rahim, A. Hermans, B. Wohlfeil, D. Petousi, B. Kuyken, D. Van Thourhout, and R. Baets, "Taking silicon photonics modulators to a higher performance level: state-of-the-art and a review of new technologies," *Advanced Photonics,* vol. 3, no. 2, p. 024003, 2021.

[2] P. J. Winzer and D. T. Neilson, "From scaling disparities to integrated parallelism: A decathlon for a decade," *JLT,* vol. 35, no. 5, pp. 1099-1115, 2017.

[3] D. A. Miller, "Attojoule optoelectronics for low-energy information processing and communications," *JLT,* vol. 35, no. 3, pp. 346-396, 2017.

[4] C. Wang, M. Zhang, X. Chen, M. Bertrand, A. Shams-Ansari, S. Chandrasekhar, P. Winzer, and M. Lončar, "Integrated lithium niobate electro-optic modulators operating at CMOS-compatible voltages," *Nature,* vol. 562, no. 7725, pp. 101-104, 2018.

[5] M. Xu, Y. Zhu, F. Pittalà, J. Tang, M. He, W. C. Ng, J. Wang, Z. Ruan, X. Tang, M. Kuschnerov, L. Liu, Y. Siyuan, Z. Bofang, and C. Xinlun, "Dual-polarization thin-film lithium niobate in-phase quadrature modulators for terabit-per-second transmission," *Optica,* vol. 9, no. 1, pp. 61-62, 2022.

[6] C. Kieninger, C. Füllner, H. Zwickel, Y. Kutuvantavida, J. N. Kemal, C. Eschenbaum, D. L. Elder, L. R. Dalton, W. Freude, S. Randel, and C. Koos, "Silicon-organic hybrid (SOH) Mach-Zehnder modulators for 100 GBd PAM4 signaling with sub-1 dB phase-shifter loss," *Optics express,* vol. 28, no. 17, pp. 24693-24707, 2020.

[7] C. Haffner, W. Heni, Y. Fedoryshyn, J. Niegemann, A. Melikyan, D. L. Elder, B. Baeuerle, Y. Salamin, A. Josten, U. Koch, C. Hoessbacher, F. Ducry, L. Juchli, A. Emboras, D. Hillerkuss, M. Kohl, L. R. Dalton, C. Hafner, and J. Leuthold, "All-plasmonic Mach–Zehnder

modulator enabling optical high-speed communication at the microscale," *Nature Photonics,* vol. 9, no. 8, pp. 525-528, 2015/08/01 2015,

[8] W. Heni, Y. Fedoryshyn, B. Baeuerle, A. Josten, C. B. Hoessbacher, A. Messner, C. Haffner, T. Watanabe, Y. Salamin, U. Koch, D. L. Elder, L. R. Dalton, and J. Leuthold, "Plasmonic IQ modulators with attojoule per bit electrical energy consumption," *Nature Communications,* vol. 10, no. 1, p. 1694, 2019/04/12 2019,

[9] M. Burla, C. Hoessbacher, W. Heni, C. Haffner, Y. Fedoryshyn, D. Werner, T. Watanabe, H. Massler, D. L. Elder, L. R. Dalton, and J. Leuthold, "500 GHz plasmonic Mach-Zehnder modulator enabling sub-THz microwave photonics," *APL Photonics,* vol. 4, no. 5, p. 056106, 2019, doi: 10.1063/1.5086868.

[10] W. Heni, B. Baeuerle, H. Mardoyan, F. Jorge, J. M. Estaran, A. Konczykowska, M. Riet, B. Duval, V. Nodjiadjim, M. Goix, J.-Y. Dupuy, M. Destraz, C. Hoessbacher, Y. Fedoryshyn, H. Xu, D. L. Elder, L. R. Dalton, J. Renaudier, and J. Leuthold, "Ultra-High-Speed 2:1 Digital Selector and Plasmonic Modulator IM/DD Transmitter Operating at 222 GBaud for Intra-Datacenter Applications," *JLT,* vol. 38, no. 9, pp. 2734-2739, 2020/05/01 2020.

[11] S. Abel, F. Eltes, J. E. Ortmann, A. Messner, P. Castera, T. Wagner, D. Urbonas, A. Rosa, A. M. Gutierrez, D. Tulli, P. Ma, B. Baeuerle, A. Josten, W. Heni, D. Caimi, L. Czornomaz, A. A. Demkov, J. Leuthold, P. Sanchis, and J. Fompeyrine, "Large Pockels effect in micro- and nanostructured barium titanate integrated on silicon," *Nature Materials,* vol. 18, no. 1, pp. 42-47, 2019/01/01 2019

[12] A. Messner, F. Eltes, P. Ma, S. Abel, B. Baeuerle, A. Josten, W. Heni, D. Caimi, J. Fompeyrine, and J. Leuthold, "Plasmonic ferroelectric modulators," *JLT,* vol. 37, no. 2, pp. 281-290, 2018.

[13] R. Germann, H. Salemink, R. Beyeler, G. Bona, F. Horst, I. Massarek, and B. Offrein, "Silicon oxynitride layers for optical waveguide applications," *Journal of the Electrochemical Society,* vol. 147, no. 6, p. 2237, 2000.

[14] Q. Wilmart, H. El Dirani, N. Tyler, D. Fowler, S. Malhouitre, S. Garcia, M. Casale, S. Kerdiles, K. Hassan, C. Monat, X. Letartre, A. Kamel, M. Pu, K. Yvind, L. K. Oxenløwe, W. Rabaud, C. Sciancalepore, B. Szelag, and S. Olivier, "A Versatile Silicon-Silicon Nitride Photonics Platform for Enhanced Functionalities and Applications," *Applied Sciences,* vol. 9, no. 2, p. 255, 2019.

[15] R. Heideman, A. Leinse, W. Hoving, R. Dekker, D. Geuzebroek, E. Klein, R. Stoffer, C. Roeloffzen, L. Zhuang, and A. Meijerink, "Large-scale integrated optics using TriPleX waveguide technology: from UV to IR," in *Photonics Packaging, Integration, and Interconnects IX*, 2009, vol. 7221: International Society for Optics and Photonics, p. 72210R.

[16] C. H. Henry, R. F. Kazarinov, H. J. Lee, K. J. Orlowsky, and L. Katz, "Low loss Si 3 N 4–SiO 2 optical waveguides on Si," *Applied optics,* vol. 26, no. 13, pp. 2621-2624, 1987.

[17] K. Ikeda, R. E. Saperstein, N. Alic, and Y. Fainman, "Thermal and Kerr nonlinear properties of plasma-deposited silicon nitride/silicon dioxide waveguides," *Optics express,* vol. 16, no. 17, pp. 12987-12994, 2008.

[18] M. H. P. Pfeiffer, C. Herkommer, J. Liu, T. Morais, M. Zervas, M. Geiselmann, and T. J. Kippenberg, "Photonic damascene process for low-loss, high-confinement silicon nitride waveguides," *IEEE Journal of selected topics in quantum electronics,* vol. 24, no. 4, pp. 1-11, 2018.

[19] A. N. R. Ahmed, S. Nelan, S. Shi, P. Yao, A. Mercante, and D. W. Prather, "Subvolt electro-optical modulator on thin-film lithium niobate and silicon nitride hybrid platform," *Optics letters,* vol. 45, no. 5, pp. 1112-1115, 2020.

[20] P. Zhang, H. Huang, Y. Jiang, X. Han, H. Xiao, A. Frigg, T. G. Nguyen, A. Boes, G. Ren, Y. Su, Y. Tian, and A. Mitchell, "High-speed electro-optic modulator based on silicon nitride loaded lithium niobate on an insulator platform," *Optics Letters,* vol. 46, no. 23, pp. 5986-5989, 2021/12/01 2021, doi: 10.1364/OL.446222.

[21] C. T. Phare, Y.-H. D. Lee, J. Cardenas, and M. Lipson, "Graphene electro-optic modulator with 30 GHz bandwidth," *Nature Photonics,* vol. 9, no. 8, pp. 511-514, 2015.

[22] K. Alexander, J. P. George, J. Verbist, K. Neyts, B. Kuyken, D. Van Thourhout, and J. Beeckman, "Nanophotonic Pockels modulators on a silicon nitride platform," *Nature communications,* vol. 9, no. 1, pp. 1-6, 2018.

[23] M. Kohli, A. Messner, T. Buriakova, P. Habegger, D. Chelladurai, T. Blatter, J. Smajic, M. Zervas, Y. Fedoryshyn, U. Koch, and J. Leuthold, "Highly Efficient Grating Coupler for Silicon Nitride Photonics with Large Fabrication Tolerance," in *OSA Advanced Photonics Congress 2021*, Washington, DC , 2021/07/26 2021: Optica Publishing Group, in OSA Technical Digest, p. IM4A.6, doi: 10.1364/IPRSN.2021.IM4A.6.

[24] J.-M. Brosi, C. Koos, L. C. Andreani, M. Waldow, J. Leuthold, and W. Freude, "High-speed low-voltage electro-optic modulator with a polymer-infiltrated silicon photonic crystal waveguide," *Optics Express,* vol. 16, no. 6, pp. 4177-4191, 2008.

[25] S. Yongqiang, Y. Lianshan, and A. E. Willner, "High-speed electrooptic modulator characterization using optical spectrum analysis," *Journal of Lightwave Technology,* vol. 21, no. 10, pp. 2358-2367, 2003, doi: 10.1109/JLT.2003.818162.

[26] D. Moor, J. Winiger, P. Ma, A. Messner, B. I. Bitachon, S. Abel, F. Eltes, J. Fompeyrine, and J. Leuthold, "> 150 GHz Hybrid-Plasmonic BaTiO3-On-SOI Modulator for CMOS Foundry Integration," in *Frontiers in Optics*, 2021: Optical Society of America, p. FTh4D. 2.